



HAL
open science

Comparing Two Strategies for Locating Hydrogen Refueling Stations under High Demand Uncertainty

Daniel Thiel

► **To cite this version:**

Daniel Thiel. Comparing Two Strategies for Locating Hydrogen Refueling Stations under High Demand Uncertainty. *Advances in Environmental and Engineering Research*, 2023, 04 (02), pp.1-21. 10.21926/aeer.2302031 . hal-04100610

HAL Id: hal-04100610

<https://hal.science/hal-04100610>

Submitted on 18 May 2023

HAL is a multi-disciplinary open access archive for the deposit and dissemination of scientific research documents, whether they are published or not. The documents may come from teaching and research institutions in France or abroad, or from public or private research centers.

L'archive ouverte pluridisciplinaire **HAL**, est destinée au dépôt et à la diffusion de documents scientifiques de niveau recherche, publiés ou non, émanant des établissements d'enseignement et de recherche français ou étrangers, des laboratoires publics ou privés.

Original Research

Comparing Two Strategies for Locating Hydrogen Refueling Stations under High Demand Uncertainty

Daniel Thiel *

CEPN, UMR-CNRS 7234, Université Sorbonne Paris Nord, 99 Avenue Jean Baptiste Clément, 93430 Villetaneuse, France; E-Mail: daniel.thiel@univ-paris13.fr

* **Correspondence:** Daniel Thiel; E-Mail: daniel.thiel@univ-paris13.fr

Academic Editor: Wendy M. Purcell

Special Issue: [Hydrogen Applications in Energy Transport and Industry: From Techno-economic, Policy, and Environmental Assessment](#)

Adv Environ Eng Res

2023, volume 4, issue 2

doi:10.21926/aeer.2302031

Received: February 21, 2023

Accepted: May 08, 2023

Published: May 15, 2023

Abstract

This research aims to model and compare two strategies for locating new hydrogen refueling stations (HRS) in a context of high uncertainty on H₂ demand and on the spatial distribution of demand points. The first strategy S1 represented by an agent-based model integrating a particle swarm optimization metaheuristic consists of finding the best HRS locations by adapting to the real evolution of the demand. A second strategy S2 consists in solving a classical capacitated p -median problem based on H₂ consumption forecasts over a given deterministic horizon in order to define in advance p optimal future HRS locations. Assuming that the same distributor gradually implements future HRSs in a given area between 2023 and 2030, both models minimize the sum of travel distances between each demand point and its assigned HRS. The results show that during the growth phase of the fuel cell electric vehicle (FCEV) market, with two different compound annual growth rates (medium and strong), the conservative S1 strategy performs better than S2 as these rates increase. However, while S2 remains suboptimal throughout the sales growth period, it becomes more effective once demand stabilizes. Another finding is that different uniform distributions of H₂ demand points in the same space have only a small long-term influence on the performance of these two



© 2023 by the author. This is an open access article distributed under the conditions of the [Creative Commons by Attribution License](#), which permits unrestricted use, distribution, and reproduction in any medium or format, provided the original work is correctly cited.

models. This research advises investors to study the influence of different location strategies and models on the performance of a final HRS network in a given region. Models can be easily configured and adapted to a particular spatial distribution of demand points in a specific environment, more flexible H₂ production capabilities, or different behaviors of FCEV drivers that could be geo-located.

Keywords

Fuel cell electric vehicle; hydrogen refueling station; step-by-step location strategy; agent-based model; particle swarm optimization; p -median model

1. Introduction

The problem of locating new hydrogen refueling stations (HRSs) is not related to the lack of optimization methods and techniques but to the high uncertainty about the sales of fuel cell electric vehicles (FCEVs) in the next few years. While waiting for more reliable forecasting models than those currently proposed by consulting firms or by researchers [1-5] who focused on the possible evolution of the number of private FCEV adopters, the current observation is that the majority of FCEVs in circulation in 2023 are public vehicles and so-called captive fleets. This is because to make HRSs cost-effective, a sufficient number of FCEVs must be on the road [6]; conversely, the FCEV market will only grow if enough HRSs available [7]. Therefore, policymakers and manufacturers have often initiated this chicken-and-egg problem by subsidizing these captive fleets. Schwoon [8] advises early HRS operators to make their investments before the H₂ demand becomes noticeable, assuming that automakers can offer competitively priced FCEVs once a core network of HRSs exists. During this start-up phase, some research has proposed optimization models for HRS locations based on a deterministic demand represented by an initial randomly distributed captive fleet [9-11]. However, once this cycle is underway, these first HRSs with excess capacity will also provide future private FCEVs with an existing infrastructure that will allow them to fuel themselves with hydrogen.

This paper addresses the location problem of new HRSs at the beginning of the growth phase of the FCEV market for private adopters and once the captive fleet is established. Knowing that the private FCEV market has just started to grow and is expected to reach its mature market phase probably in a few decades, two progressive HRS location strategies are modeled taking into account different degrees of uncertainty on the volumes of H₂ demand to be supplied and on the geographical location of the demand points. The objective of this research is to compare a cautious investment strategy S1 which consists in locating each new HRS in order to adjust the H₂ capacity to the uncertain demand with a strategy S2 that chooses to place each HRS on one of the p sites calculated by an optimization model which will allow to supply the estimated demand at the end of the growth period. S1 also seeks to locate each new HRS in such a way as to absorb the additional demand by positioning itself as far away as possible from the other HRSs to cover the territory extensively in order to satisfy as many customers as possible and to avoid as much as possible future price competition between HRSs ([9] see also [12, 13] proposing the p -dispersion problem that maximizes the minimum distance between any pair of facilities). S2 is based on a p -median model

[14] which minimizes the sum of the distances between the demand points and their allocated HRS. When the number of FCEVs on the road stabilizes, the final locations of the p HRSs should be optimal by following S2. S1 is a more conservative strategy in the face of demand uncertainties. It seeks to optimize the location of each HRS one after the other, taking the risk that the final location of the p HRS is not optimal at the end of the market growth phase.

The manuscript is organized as follows. Section 2 presents state of the art on the different methods and models for locating HRSs and the empirical assumptions made on H₂ demand by different authors. This review selects and presents two mathematical location models in Section 3. Section 4 describes a case study that considers two types of demand uncertainty, one related to estimates of the forecasted volume of H₂ to be supplied over a given time horizon and the other, explained by various possibilities for the geographic distribution of future demand points. Section 5 compares the performance of the two HRS location models. A conclusion in Section 6 summarizes the main results, indicates how this research contributes to the current literature, and presents its contribution in decision support for implementing new HRSs in a still uncertain FCEV market.

2. Literature Review

2.1 Approaches and Models for Locating Hydrogen Refueling Stations

In order to position and justify the two models used in this paper, research on HRS location published between 2003 and 2022 was first classified into three types of methods and models (see Table 1): (i) Empirical research and multi-criteria decision-making models, (ii) Mathematical programming models, (iii) Simulation and metaheuristics algorithms.

Table 1 HRS location approaches and models proposed in the literature.

Ref.	Empirical research Multi-criteria decision-making models	Ref.	Mathematical programming models	Ref.	Simulation Metaheuristics algorithms
[15]	Empirical proposals for HRS locations	[16]	p -center and p -median models	[17]	Simulation model
[18]	Multi-criteria decision-making Analytic hierarchy process	[19]	Flow-refueling location model	[20]	Particle swarm optimization
[21]	Multi-criteria decision-making	[22]	p -median model Flow-refueling location model	[8]	Agent-based model
[23]	Empirical study searching for suitable HRS places	[24]	Flow-refueling location model Mixed-integer linear programming	[25]	Genetic algorithm Greedy algorithm Simulated annealing algorithm
[26]	Fuzzy multi-criteria decision-making	[27]	Flow-refueling location model	[9]	Agent-based model Particle swarm optimization

[28] Multi-criteria decision-making	[29] p -center flow-refueling location model	[30] Multi-objective model Particle swarm optimization
	[31] p -median model Cost-based model Risk-based model	Analytic hierarchy process
	[32] Population-based model Goal programming model Maximum coverage	[33] Fuzzy comprehensive evaluation method Artificial neural network model
	[34] model p -median model	
	[35] Lagrange relaxation algorithm model	
	[36] Set covering model Multi-objective model	
	[10] Iterative polynomial-time approach	

Empirical research using multi-criteria decision-making methods is positioned in very different environments with territorial specificities and a great diversity both in H₂ production technologies and in the expectations of FCEV drivers located or circulating in specific spaces. For these reasons, these empirical approaches in varying contexts are difficult to compare. Optimization models have the advantage of using the same mathematical formalism, thus facilitating comparisons, which is the aim of our research. Mathematical programming applied to facility location is based on either a point demand approach (demand is located at specific locations) or a flow demand approach (consumers seek to refuel at an HRS on their way to their final destination). In the case of a point demand approach, many authors solve the p -median or *minimum* problem or the covering problem [37]. In a demand-flow approach, the models seek to optimally locate HRSs along the routes taken by FCEVs [19]. Of these works searching for the best HRS locations, only Upchurch & Kuby [22] compared the performances of two HRS location models. Their research showed that HRS located by the flow-refueling model generally perform better on the p -median objective than HRSs located by the p -median model on the flow-refueling objective. Moreover, the optimal locations for the flow-refueling model tend to be much more stable as p increases than those located by the p -median model.

Our research aims to compare the classical p -median model which is NP-hard with a particle swarm optimization (PSO) metaheuristic approach [38] formulated within the framework of an agent-based model [39] that is easily parameterized and capable of incorporating nonlinear constraints, if needed, in practical applications. PSO is a population-based metaheuristic based on the collaboration of individuals (particles) between them and on the concept of self-organization. The particles progressively converge towards a global minimum corresponding to an HRS's best location by setting simple displacement rules.

2.2 Assumptions Made About H₂ Demand

The models for locating HRSs in a given space use data on the H₂ volume that needs to be supplied and the spatial distribution of the demand points. The assumptions made by the various authors regarding these data are either deterministic or stochastic. Some research relies on estimates of H₂ consumption histories in regions [31-33] and explanatory statistical models [40]. Many works estimate H₂ demand based on actual geographic information system (GIS) data showing the location of existing road structures and gas stations. Some also rely on FCEV private owners' spatial distribution and typology in a given area [3, 4, 12-16, 22, 27, 29, 33, 39]. However, predicting FCEV sales is difficult and complex due to the unavailability of past data. To overcome this problem, some researchers use the Bass adoption and diffusion model [27] or discrete choice models [41]. Other researchers model demand uncertainty using fuzzy concepts [35, 36] or a scenario-generating stochastic model for FCEV demand based on vehicle driving behavior and different FCEV models [42]. Some work also considers distance or travel time uncertainties and solves a stochastic p -median problem [38-40]. Berman and Drezner [43] develop a progressive p -median model under uncertainty which assumes that demand will increase uniformly at all demand points, leading to the implementation of new facilities. Also, in a case study of emergency service location, Shetab-Boushehri et al. [44] introduce uncertainty in the location of demand points by estimating the number of requests for assistance based on a history of the number of calls per point in the study area.

This literature review has highlighted various approaches and methods for solving HRS location problems showing their applicability in many real cases. However, the numerical results often depend on the hypotheses formulated to estimate the H₂ demand, which leads us to direct our research toward a comparison of two optimization models. Using the same dataset, their reciprocal results will be compared by subjecting them to uncertainties in both the volume of H₂ demand (U1) and the randomness of the spatial distribution of demand points (U2).

3. Model Description

This section is organized as follows.

Subsection 3 presents two location optimization models:

- The first formal model of the step-by-step strategy S1 is a gradual and cautious approach to implementing HRSs during the growth phase of the H₂ demand (see §3.1.1).
- The second model represents the strategy S2 of optimizing the location of p HRSs needed to meet total demand at the end of a given period T . Each HRS is located incrementally as the volume of demand increases only among one of the p possible optimal locations (see §3.1.2).

Subsection §3.2 presents the global model integrating the two optimization models. It evaluates the performance from $t = 1$ to T through the cumulative distances between the demand points to be supplied by the nearest available HRS.

Subsection §3.3. outlines the model parameters representing demand uncertainties.

3.1 HRS Location Optimization Models

3.1.1 Step-By-Step Location Model S1

This strategy aims to satisfy as many clients as possible by creating a network of HRSs that is as extensive as possible to avoid concentrating supply in the center of a territory. By dispersing the HRSs as much as possible, it will also limit the effect of subsequent price competition between HRSs. An agent-based model and a PSO algorithm are developed seeking on the one hand to disperse these HRSs as best as possible (i.e., seeking to maximize the sum of distances between all pairs of HRSs) and on the other hand to locate them as close as possible to a sufficient number of customers in order to ensure the return on investment (as proposed by [44] by setting profitability thresholds required by investment in HRSs). In the model, HRSs gradually reach a saturation point as H₂ demand increases.

Agent-Based Model. The model is based on the following principle:

- Each cell in the square region R under study represents the possible placement of an agent.
- The locations of the H₂ demand points (passive agents) are randomly positioned in R .
- A first HRS (passive agent) is positioned in the center of the square.
- n active agents (PSO particles) are generated and randomly placed in R .

To implement each new HRS *step-by-step*, the model compares the distances between the demand points and each HRS and tries to implement the new HRS as far as possible from the existing HRSs.

Local Search Heuristics. The heuristic is based on the PSO algorithm which initiates the movement of the particles step-by-step based on three components: their current velocity V , their best solution, and the best solution obtained in their neighborhood. Each particle representing a possible location of the new HRS, will attract a demand point only if the distance is smaller than the distance of the already installed HRSs. As long as the number of FCEVs to be served is less than the minimum number of FCEVs to ensure a good return on investment of the new HRS, the PSO algorithm searches for a location by moving closer to another HRSs. The model stops when the number of FCEVs choosing the new HRS is sufficient and the other HRSs do not exceed their maximum capacity.

PSO Pseudo-Code. Each HRS location has a *quality* determined by the objective function to be minimized, corresponding to the total cumulative distance between all demand points and the HRS. The algorithm consists of five steps described below:

1. Each particle k has a current position (X_k, Y_k) in R , a given velocity V_k . Its best position is stored at coordinates (BX_k, BY_k) . All particles know the particle g that found the best location, so that (BX_g, BY_g) is the best possible location among all.
 $X_k := BX_k$ and $Y_k := BY_k$ //initial position of the best location.
 $BX_g := X_h$ and $BY_g := Y_h$ //position of a particle h chosen at random among the n particles.
2. The velocity and position of the particles evolve according to the following rules:

$$V_k' := \omega V_k + \varphi_1 ((BX_k - BY_k)^2 + (X_k - Y_k)^2)^{1/2} + \varphi_2 ((BX_g - BY_g)^2 + (BX_k - BY_k)^2)^{1/2}$$

where ω is an inertia parameter, φ_1 and φ_2 are random numbers uniformly distributed in $[0, 2]$.

$$X_{k'} := X_k + V_{k'}$$

$$Y_{k'} := Y_k + V_{k'}$$

3. Calculate the cumulative Euclidian distance Z between the particle located in $(X_{k'}, Y_{k'})$ which corresponds to a possible interesting HRS location and all the nearest customers who will travel to fill up with H_2 (within the capacity of this HRS).
4. **For** $k: = 1$ to n .

if $Z(X_{k'}, Y_{k'}) < Z(BX_k, BY_k)$ then $Z(BX_k, BY_k) := Z(X_{k'}, Y_{k'})$ **end if**

if $Z(BX_k, BY_k) < Z(X_g, Y_g)$ then $Z(X_g, Y_g) := Z(BX_k, BY_k)$ **end if**

Next k

5. Back to step 1, the algorithm stops after a fixed number of iterations.

3.1.2 Location Optimization Model S2

The problem of the capacitated p -median problem is solved based on a deterministic stable demand D_{max} corresponding to the end of the growth cycle of the FCEV market at the end of a period T . From the set of possible locations of HRSs on the same region R , the model will have to search for the optimal location of p HRSs that will be able to supply the total demand D_{max} to minimize the sum of the distances between each point of demand and its assigned HRS, knowing that each HRS is limited in capacity and will therefore be able to serve only a limited number of FCEVs. This problem is solved according to [45] who propose an algorithm using *Lagrangian* relaxation, to group n entities into p mutually exclusive and exhaustive groups where the capacity of each group is limited. Once the p locations of the HRSs are fixed, each new HRS will be chosen only from one of the p optimal locations. As in the S1 strategy, the HRSs gradually reach a saturation point as the H_2 demand increases.

Mathematical Formulation of the Capacitated p -median. The goal is to determine the location of p HRSs in an $r \times r$ grid space R with r^2 candidate locations to satisfy a set of D_{max} demand points (i.e., the location of D_{max} FCEVs).

Knowing that each HRS can only supply a limited number of FCEVs and that each customer is only assigned to one HRS, the problem consists in minimizing the sum of the distances between each demand point and its allocated HRS.

$$\text{Minimize } Z := \sum_{i=1}^{D_{max}} \sum_{j=1}^{r^2} a_{ij} d_{ij}$$

where $i := 1, 2, \dots, D_{max}$ is the set of demand points, $j = 1, 2, \dots, r^2$ the set of possible locations of the p medians, m the same H_2 volume demand for each customer i , K the same capacity of each HRS j , $d_{ij} \geq 0$ the distance between an FCEV i and an HRS j and the decision variable.

$$a_{ij} := \begin{cases} 1, & \text{if a FCEV } i \text{ is assigned to the HRS } j \\ 0, & \text{otherwise} \end{cases}$$

s.t.

$\sum_{i=1}^{Dmax} a_{ij} := 1, j = 1, 2, \dots, r^2$ // Constraints which impose that each FCEV is assigned to one and only one HRS.
 $\sum_{i=1}^{Dmax} m a_{ij} \leq K, j = 1, 2, \dots, r^2$ // Constraints that prevents exceeding a maximum HRS capacity.
 $\sum_{i=1}^{Dmax} \sum_{j=1}^{r^2} a_{ij} = p$ // Constraint to ensure that p medians will be located.
 $a_{ij} \in \{0, 1\} \forall i, j$ // Integer constraint.

3.2 Global Model Assessing the Performance

3.2.1 Pseudocode

Input

T := Time to reach the maturity threshold of the FCEV market.
 T := Discrete time increasing between 0 and T with a step dt of one day.
 K := Market growth scenario, $k = 1$ (average sales growth) or $k = 2$ (strong sales growth).
 $D_k(t)$:= Number of FCEVs to be served in H_2 per day following a market evolution curve for each scenario k .
 $Dmin$:= Initial number of FCEVs ($D_k(t) := Dmin$).
 $Dmax_k$:= Stable demand to be satisfied in the mature market phase ($Dmax_k := D_k(T)$).
 $CAGR$:= Compound annual growth rate.
// Each scenario k represents a possible evolution of the demand curve $D_k(t)$ during the market growth phase, which is assumed to evolve exponentially. Different possible $CAGR$ values correspond to the first uncertainty U1 on demand. At the end of a period T corresponding to the beginning of the maturity phase of the FCEV market, $D_k(T)$ will reach a stable demand $Dmax_k$ of H_2 to be supplied per day.
// In addition, the model also considers the daily demand $D_k(t)$ is randomly and uniformly distributed between 0 and T in the same bounded space R which allows us to simulate an uncertainty U2 on the location of the demand.
 K := Maximum HRS capacity in kg H_2 /day.
 m := Mass of H_2 in kg at a pressure of 200 bars to refuel an FCEV with a three-quarter empty tank.
// It is assumed that FCEVs drive through the region R daily and decide to refill their tanks as soon as the fuel gauge is at $\frac{1}{4}$ level. Depending on where they are when the gauge reaches this level, they will seek to refuel at the nearest HRS.

Other variables

$Nmax_k$:= Total number of HRSs installed at the end of the growth period ($Nmax_k = N_k(T)$).
 $N_k(t)$:= Number of HRSs at time t .
 d_{ij} := Distance between FCEV i and HRS j .

Output

$Z_k(t)$:= Sum of the distances between HRS i and FCEV j at time t for each scenario k .
 $TD_k(t)$:= Cumulative distance traveled by FCEVs at time t to refuel at the nearest HRS for each scenario k .

Procedure

For each scenario k of demand evolution ($k := 1$ or 2).

$D_k(0) := D_{min}$ // The initial number of FCEVs.

$TD_k(0) := 0$.

$N_k(0) := 1$ // A first HRS is located in the middle of the region R .

$N_{max_k} := [mD_{max_k}/K]$

For $t := 1$ to T step $dt := 1$ (every day).

$D_k(t) := (1 + CAGR) D_k(t - 1)$

if $mD_k(t) > K$ **then**

// For $k := 1$, search for the best location of a new HRS following the strategy S1 and allocating the demand nodes i to the HRS j (see the model description in §3.1.1).

// For $k := 2$, since $p := N_{max_2}$ optimal HRS locations are already computed by the model S2 (see §3.1.2), only the $N_2(t)$ HRSs closest to the current $D_2(t)$ customers at time t will be selected from $p := N_{max_2}$.

$N_2(t) := N_2(t) + 1$

// Whenever the total volume of demand $D_k(t)$ exceeds the capacity supplied by the already installed HRSs, a new HRS will be installed for $k := 1$ or chosen among the $(N_{max_2} - N_2(t))$ HRSs not yet selected for $k := 2$.

end if.

// Calculate the sum of the distances between FCEV i and HRS j .

$Z_k(t) := (\sum_{i=1, N_k(t)} \sum_{j=1, D_k(t)} d_{ij})$.

// Calculate the cumulative distances.

$TD_k(t) := TD_k(t) + Z_k(t)$.

Next k

3.3 Model Parameters Representing Demand Uncertainties

The parameter CAGR allows the simulation of different exponential growths in demand and represents the uncertainty U1 on the number $D_k(t)$ of FCEVs to be served in H_2 .

$$D_k(t) := (1 + CAGR) D_k(t-1) \text{ with } D_k(0) = D_{min}.$$

The uncertainty U2 corresponding to the location of the demand points in the space R is simulated using a random number generator which modifies the spatial distribution according to the same 2-dimensional uniform distribution law each time.

4. Case Study

4.1 Modeling Assumptions

The research's various assumptions about future H_2 demand are presented in §2.2. are mostly validated in the context of a specific environment such as a city, region or bounded territory. In this case study, a theoretical space has been chosen in which the demand points are randomly distributed. Numerous estimates of FCEV sales are also published regularly in the trade press, showing large differences in both the projected medium- and long-term FCEV fleet and the number

of HRSs to be expected¹. Three research firms have conducted market studies to estimate global FCEV sales between 2023 and 2031² assuming growth takes place at an exponentially compounded annual rate (CAGR)³. On this basis, two scenarios were proposed, presented in Table 2.

Table 2 Projected FCEV sales growth rates between 2023 and 2031.

Scenarios	CAGR
$k = 1$	0.4432
$k = 2$	0.595

It was also assumed that at the beginning of 2023, the initial H_2 demand $D_k(0) = 9$ FCEVs to be served per day and that only one HRS was already implemented. Depending on the CAGR values for each scenario k , the final demand at the end of 2031 would be $D_{max1} = 160$ or $D_{max2} = 360$ FCEVs to serve per day. The graph in Figure 1 represents the daily evolution of demand $D_1(t)$ which corresponds to "average" sales growth and $D_2(t)$ to higher sales growth between $t = 0$ (the year 2023) and $T = 2920$ days (the year 2031).

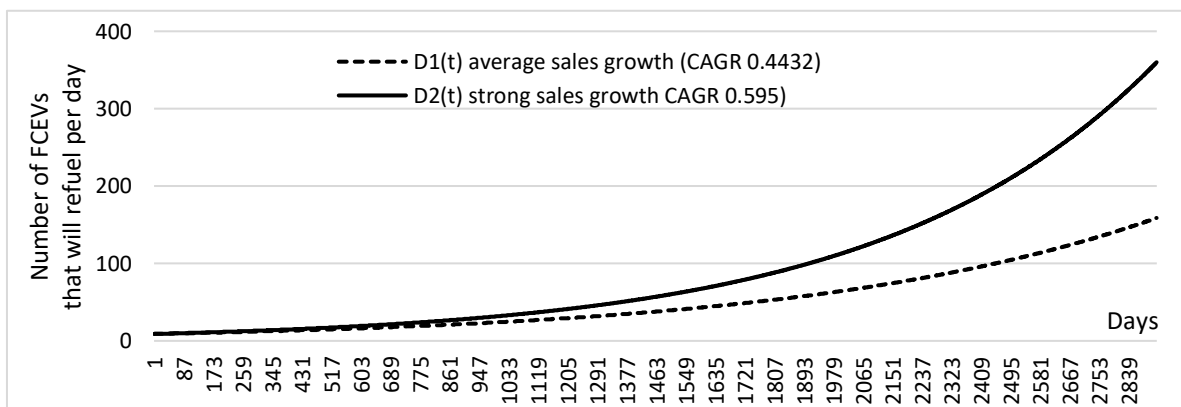


Figure 1 Number of FCEVs per day to be supplied with H_2 from 2023 to 2031.

It is considered in this study that HRSs have the same capacity and are implemented by the same distributor without price competition. A station that uses H_2 in the form of gas, has a maximum capacity $K = 200$ kg/day. It is also assumed that an FCEV (excluding taxis and professional vehicles) travels on average 36 kms per day and based on the average consumption of *Mirai* or *Nexo*-type cars of 0.80 kg H_2 per 100 km, this would correspond to an average consumption per day of 0.29 kg/day/FCEV. Since the range is about 600 kms and each FCEV will head to an HRS to refuel as soon as it has covered 450 kms ($\frac{1}{4}$ gauge left), each FCEV will go on average to refuel every 12.5 days. Knowing that the content of the tank of a sedan-type FCEV is about 5.8 kg H_2 , the filling of H_2 corresponds to about 4.36 kg. An HRS can therefore serve a maximum of 45 FCEV per day. This

¹ <https://www.transportenergystrategies.com/2022/05/03/hydrogen-targets-v-actual-sales-theres-a-gap/>
<https://www.degruyter.com/document/doi/10.1515/eng-2021-0039/html>

² Frost & Sullivan, July, 2015 <https://www.frost.com/frost-perspectives/fuel-cell-electric-vehicles-genesis-new-era-or-myth-busting-new-energy-vehicle-technology>
 Precedence Research, May, 2022 <https://www.precedenceresearch.com/press-release/fuel-cell-market>
 Research and Markets, September, 2021, <https://www.researchandmarkets.com/reports/5447674/fuel-cell-vehicle-market-global-forecast-2021>

³ A sigmoid function could also have been chosen to represent the growth phase of the market until its maturity.

means that if $D_{max_1} = 160$ or $D_{max_2} = 360$, the total number of FCEVs on the same territory R at time $T = 2920$ days will be 2,000 for scenario $k = 1$ or 4,500 FCEVs for $k = 2$. Moreover, it is assumed that an HRS can serve about 40 FCEVs per day, i.e., $40 \times 4.36 = 174$ kgs of H_2 (for a theoretical capacity of 200 kg/day).

4.2 Experimentation Protocol

The region R is represented by a square of 3.6 km side length. The performance of the two models is compared based on the Euclidean distances traveled between each demand point and its assigned HRS. The uncertainty U1 on the volume of forecasted demand in H_2 is represented by the two scenarios k . The uncertainty U2 on the geographical location of demand points is simulated by randomly distributing demand points in the region R (by using a uniform distribution on the two-dimensional set).

To model the strategy S1, a 36×36 gridded space is developed using the NetLogo 6.3.0 programmable multi-agent modeling environment [46]. This square space contains 576 cells corresponding to all possible locations of the agents (H_2 demand points or HRSs) whose number progresses in time according to the chosen scenario k until reaching D_{max_k} .

To model S2, the IBM ILOG CPLEX 12.9 solver is chosen to solve the capacitated p -median problem.

5. Results and Discussion

The performance of the two strategies is compared as a function of the uncertainty U1 on estimated FCEV sales between 2023 and 2030 (§5.1). Then, the influence of the uncertain distribution of demand points U2 in the studied space R (§5.2) and the limitations of this research (§5.3) are presented.

5.1 Influence of Demand Uncertainty U1 on the Optimized HRS Locations

For each scenario k of possible demand evolution (cf. uncertainty U1), the following figures show the locations of HRSs (represented by a black square in the grid) as a function of the number of FCEVs (small black cars in the grid) randomly distributed in the space R .

Following S1 strategy, Figure 2 shows different final locations of 4 HRSs at the end of period T for an average sales growth of the FCEVs market ($k = 1$) and Figure 3 the suggested location of 9 HRSs in case of strong sales growth ($k = 2$).

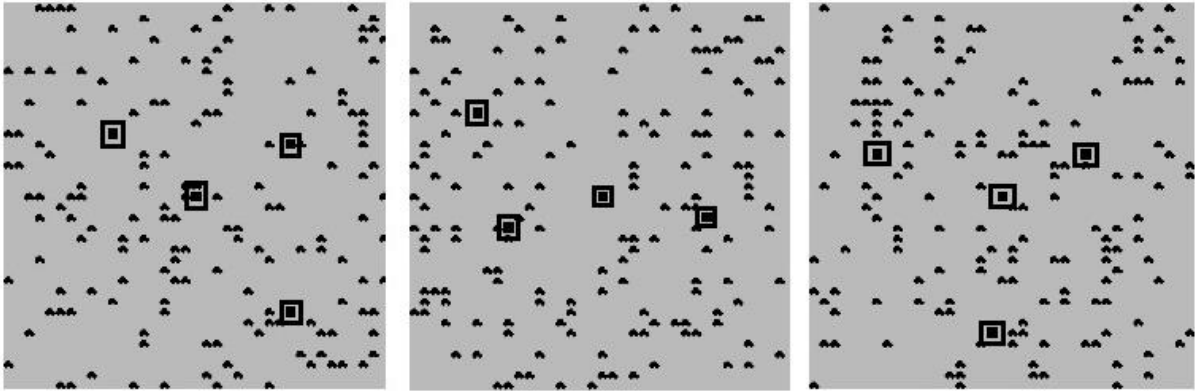


Figure 2 Step-by-step location strategy S1 for the scenario $k = 1$ of average sales growth.

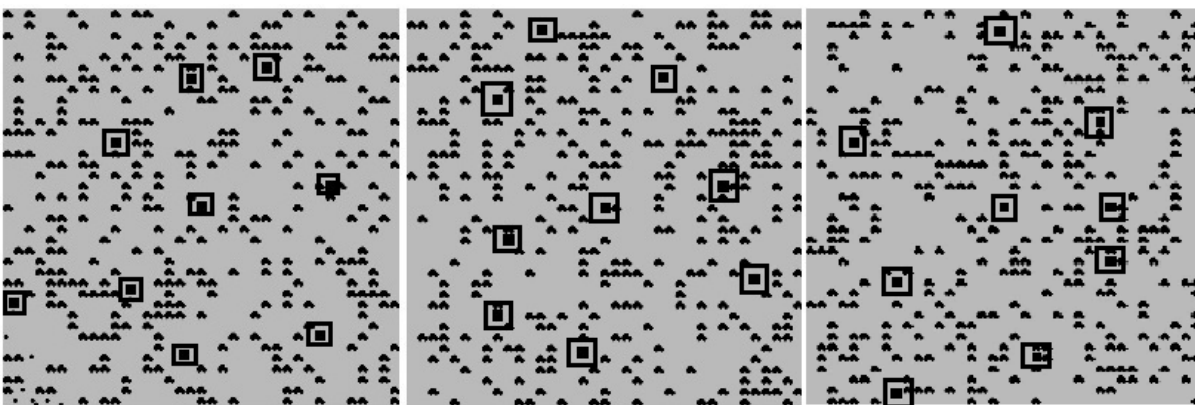


Figure 3 Step-by-step location strategy S1 for the scenario $k = 2$ of strong sales growth.

Figure 4 and Figure 5 show the evolution of the location of HRSs during the period from 0 to T for each scenario k by choosing the optimal S2 location strategy based on a forecasted demand D_{max} at $t = T$.

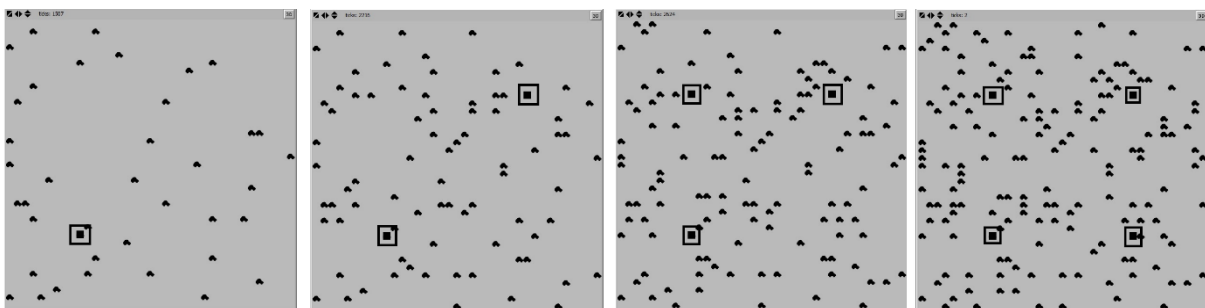


Figure 4 p -median location strategy S2 for the scenario $k = 1$ of average sales growth.

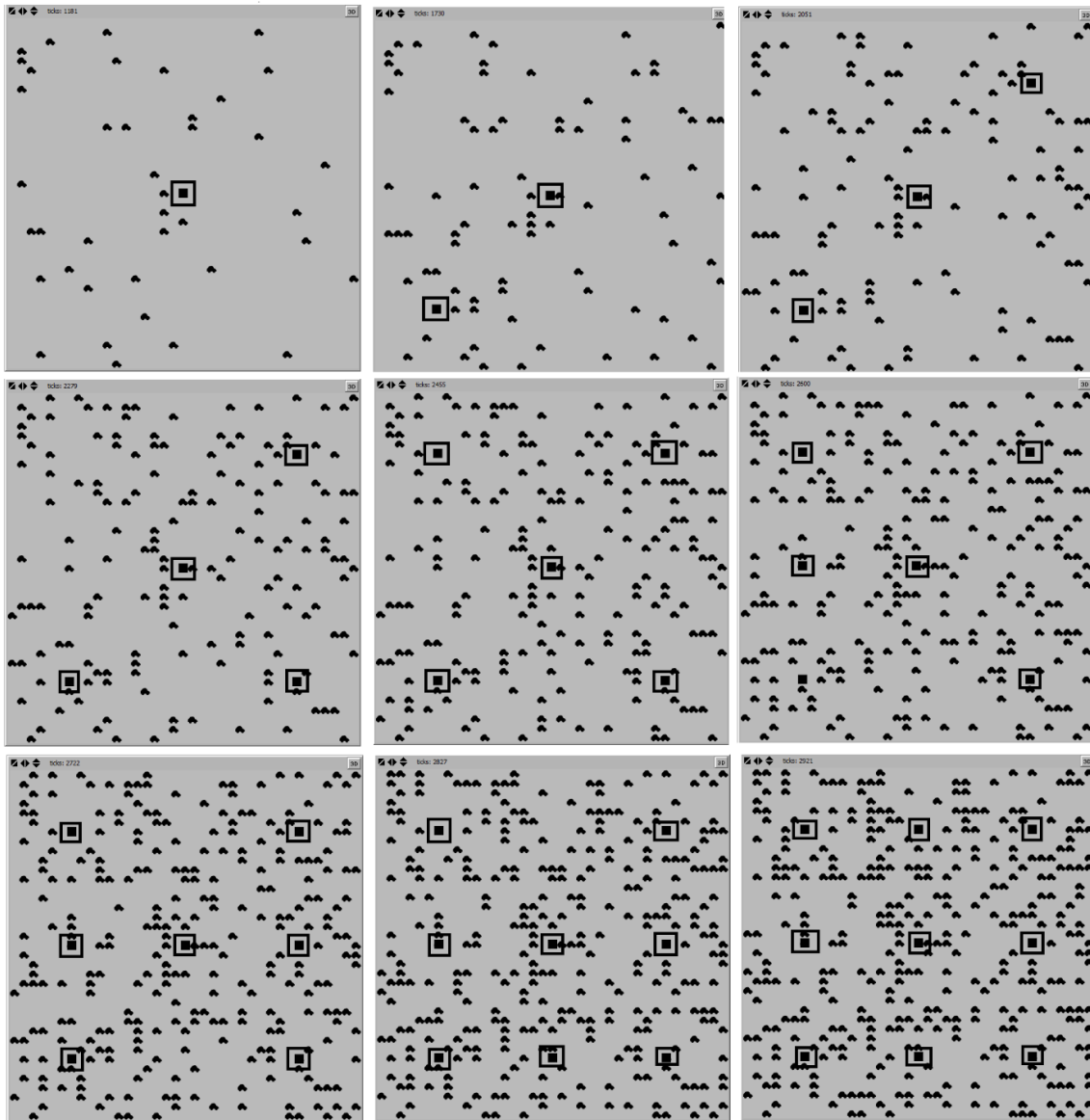


Figure 5 p -median location strategy S2 for the scenario $k = 2$ of strong sales growth.

Figure 6 shows the differences in performance between S1 and S2 calculated by summing the distances between each demand point and its assigned HRS for each scenario k . It can be seen that S1 is more interesting during the period of growth of the FCEVs fleet until T whatever the scenario k of sales evolution. The stronger the growth, as for $k = 2$, the more interesting the performance of S1 is during this period but the gap is rapidly reduced until $T = 2.920$ days (8 years). After the growth period, if the market stabilized with an average daily demand $Dmax_k$, it is found that for $k = 2$, S2 aiming at the optimal location of HRSs, becomes very quickly more interesting than S1 from 2,930 days. In contrast, if the demand grew less quickly, S2 becomes more interesting only from 3,100 days.

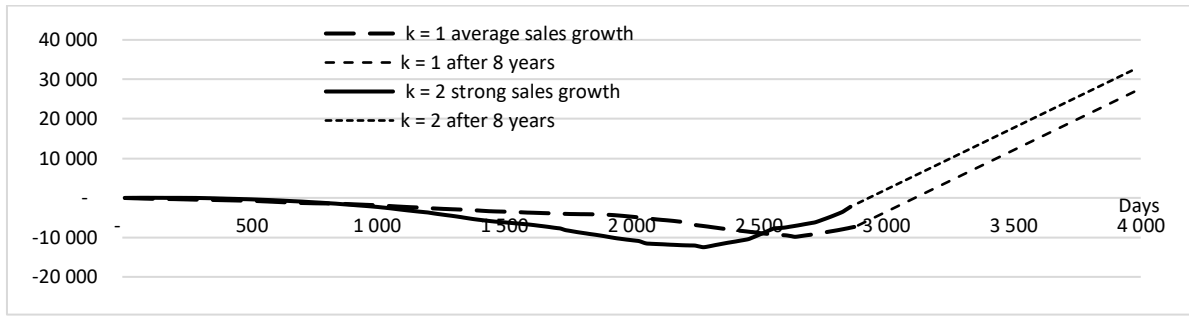


Figure 6 Differences in performance between S1 and S2 location strategies.

Figure 7 shows the cumulative distances and indicates that after about 4,000 days or nearly 3 years after the end of market growth ($T = 8$ years) that S2 will be more attractive than S1 for both scenarios $k = 1$ and $k = 2$.

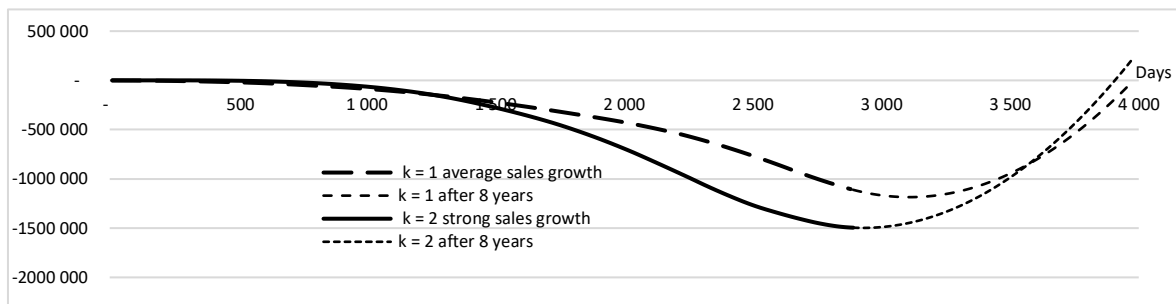


Figure 7 Cumulative differences in performance between S1 and S2 location strategies.

5.2 Influence of Demand Uncertainty U_2 on the Optimized HRS Locations

To study the influence of future demand point locations, several scenarios are simulated by randomly distributing them according to a two-dimensional uniform distribution in the same region R . Figure 8 shows the coefficients of variation in % (ratio of the standard deviation to the mean) of the total distances calculated by the two models S1 and S2 for about 100 demand point location scenarios. It can be seen that whatever the random distribution of demand in R , the gap progressively decreases by about 17% to reach 5% after $T = 8$ years, which shows that over a fairly long period, the different possible locations of the demand points have an influence on the performance of the S1 or S2 strategic choices of HRS locations that decreases with time.

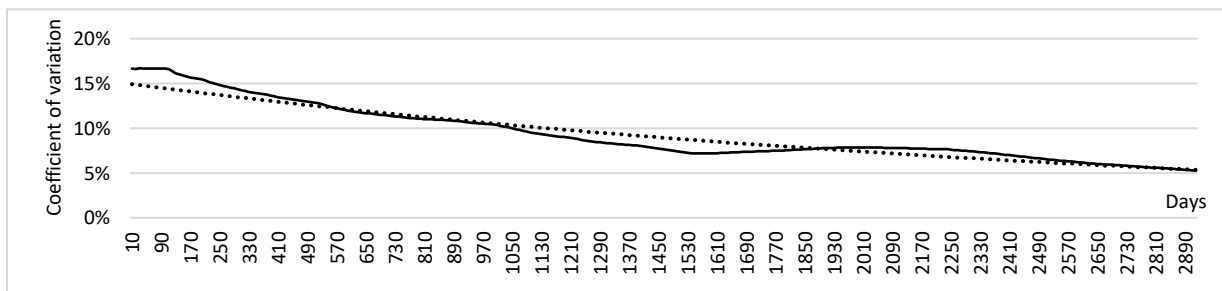


Figure 8 Differences in the distances computed by S1 and S2 as a function of the random locations of FCEVs in R .

5.3 Research Limitations

5.3.1 Limitations on the Assumptions Made About Demand

The demand points were distributed in space following a uniform distribution. Empirical studies on the routes of FCEVs, on the location of households and other factors such as age and income (see references in §2.2) could allow a more realistic statistical distribution of future H₂ demand points. A flow demand approach could also be proposed by identifying trips by cars seeking to refuel at an HRS on the way to their final destination.

It is also assumed that the market evolves exponentially to reach a demand D_{max} at the end of a long period T . The logistic function, an S-shaped curve is more common to illustrate the progression of the diffusion of an innovation.

The S2 strategy is very sensitive to sales forecasts because it assumes a stabilization of the market at the end of a given period in order to determine p optimal locations.

5.3.2 Limitations on the Assumptions Made About the HRS Capacity

In our models, each HRS has the same capacity K of up to 200 kg H₂/day which can be obtained for example, by steam methane reforming with CO₂ capture and storage. However, new production technologies are also available, such as green hydrogen produced from renewable energy and water electrolysis [35, 47, 48] which has become a good alternative for the energy transition and provides greater capacity diversity and flexibility.

6. Conclusion

There is still a great deal of uncertainty about the evolution of the number of private FCEV adopters, which explains the difficulty of locating HRSs on such uncertain grounds. Our models can provide an answer to a concrete question for investors: should they adopt a conservative strategy S1 to optimize the location of a new HRS as soon as real demand justifies it, or should they choose to locate each HRS in one of the p optimal locations calculated *a priori* from forecasted demand over a given time horizon (cf. S2 strategy). The observed results show that S1 is preferable to S2 the higher the market growth rate, which might encourage decision makers to choose S1 in the event of high uncertainty about FCEV sales. Conversely, the higher the growth rate, the more quickly the S2 strategy will become profitable once the market matures. On the other hand, the suboptimal choice S1 would probably lead to a spatial readjustment of HRSs in the future with the resulting economic losses.

This research can also enrich the current literature by comparing the performance of two location models based on the same dataset with two types and levels of demand uncertainties (uncertainties on the volume of H₂ to supply and on the spatial distribution of customers). Furthermore, an agent-based approach incorporating optimization metaheuristics is also not, to our knowledge, widely used in current research to solve facility location problems (see [49]). It allows to easily represent a given space and the interactions between the agents, which is complex or even impossible using mathematical programming.

7. Research Outlooks

To foster the transition to carbon neutrality, new HRS technologies can also help increase the flexibility of H₂ production capacities to enrich our models. It is quite possible to consider a variable capacity K_j for each HRS j that will be arbitrarily and *a priori* fixed by the decision makers and that the p median model will try to locate as well as possible. In addition, it is possible to solve a bi-objective optimization problem aimed at defining the number p of HRSs to be launched and to estimate K_j for each HRS $j = 1, 2, \dots, p$ (see [50]). The consideration of other factors can also be integrated into the models after a study of FCEV drivers' behaviors in their choice of a station and the distances they travel when they decide to fill up (with an appropriate metric). Spatial representations of demand points can be based on GIS data.

Acknowledgments

This work was conducted as part of the projects LabEx MME-DII (French National Research Agency).

I would like to thank the three anonymous reviewers for their time and effort in reviewing this paper.

Author Contributions

The author did all the research work of this study.

Competing Interests

The author has declared that no competing interests exist.

References

1. Kurtz J, Bradley T, Winkler E, Gearhart C. Predicting demand for hydrogen station fueling. *Int J Hydrog Energy*. 2020; 45: 32298-32310.
2. Saritas O, Meissner D, Sokolov A. A transition management roadmap for fuel cell electric vehicles (FCEVs). *J Knowl Econ*. 2019; 10: 1183-1203.
3. Staffell I, Scamman D, Abad AV, Balcombe P, Dodds PE, Ekins P, et al. The role of hydrogen and fuel cells in the global energy system. *Energy Environ Sci*. 2019; 12: 463-491.
4. Xu C, Wu Y, Dai S. What are the critical barriers to the development of hydrogen refueling stations in China? A modified fuzzy DEMATEL approach. *Energy Policy*. 2020; 142: 111495.
5. Khan U, Yamamoto T, Sato H. Understanding attitudes of hydrogen fuel-cell vehicle adopters in Japan. *Int J Hydrog Energy*. 2021; 46: 30698-30717.
6. Köhler J, Wietschel M, Whitmarsh L, Keles D, Schade W. Infrastructure investment for a transition to hydrogen automobiles. *Technol Forecast Soc Change*. 2010; 77: 1237-1248.
7. Ball M, Weeda M. 11-The hydrogen economy-vision or reality? In: *Compendium of hydrogen energy*. Oxford: Woodhead Publishing; 2016. pp. 237-266.
8. Schwoon M. A tool to optimize the initial distribution of hydrogen filling stations. *Transp Res D*. 2007; 12: 70-82.

9. Thiel D. A pricing-based location model for deploying a hydrogen fueling station network. *Int J Hydrog Energy*. 2020; 45: 24174-24189.
10. Kim H, Kim BI, Thiel D. Exact algorithms for incremental deployment of hydrogen refuelling stations. *Int J Hydrog Energy*. 2021; 46: 28760-28774.
11. Zhao T, Liu Z, Jamasb T. Developing hydrogen refueling stations: An evolutionary game approach and the case of China. *Energy Econ*. 2022; 115: 106390.
12. Erkut E. The discrete p-dispersion problem. *Eur J Oper Res*. 1990; 46: 48-60.
13. Kuby MJ. Programming models for facility dispersion: The p-dispersion and maximum dispersion problems. *Geogr Anal*. 1987; 19: 315-329.
14. Daskin MS, Maass KL. The p-median problem. In: *Location science*. Cham: Springer International Publishing; 2015. pp. 21-45.
15. Melaina M. Initiating hydrogen infrastructures: Preliminary analysis of a sufficient number of initial hydrogen stations in the US. *Int J Hydrog Energy*. 2003; 28: 743-755.
16. Nicholas MA, Handy SL, Sperling D. Using geographic information systems to evaluate siting and networks of hydrogen stations. *Transp Res Rec*. 2004; 1880: 126-134.
17. Tachikawa Y, Sugiura T, Shiga M, Chiyo R, Sasaki K. Numerical analysis of the optimal distribution of hydrogen filling stations. In: *Hydrogen Energy Engineering*. Tokyo: Springer; 2016. pp. 581-586.
18. Messaoudi D, Settou N, Negrou B, Rahmouni S, Settou B, Mayou I. Site selection methodology for the wind-powered hydrogen refueling station based on AHP-GIS in Adrar, Algeria. *Energy Procedia*. 2019; 162: 67-76.
19. Kuby M, Lines L, Schultz R, Xie Z, Kim JG, Lim S. Optimization of hydrogen stations in Florida using the Flow-Refueling Location Model. *Int J Hydrog Energy*. 2009; 34: 6045-6064.
20. Sun H, He C, Wang H, Zhang Y, Lv S, Xu Y. Hydrogen station siting optimization based on multi-source hydrogen supply and life cycle cost. *Int J Hydrog Energy*. 2017; 42: 23952-23965.
21. Zhou J, Wu Y, Tao Y, Gao J, Zhong Z, Xu C. Geographic information big data-driven two-stage optimization model for location decision of hydrogen refueling stations: An empirical study in China. *Energy*. 2021; 225: 120330.
22. Upchurch C, Kuby M. Comparing the p-median and flow-refueling models for locating alternative-fuel stations. *J Transp Geogr*. 2010; 18: 750-758.
23. Karipoğlu F, Serdar Genç M, Akarsu B. GIS-based optimal site selection for the solar-powered hydrogen fuel charge stations. *Fuel*. 2022; 324: 124626.
24. MirHassani SA, Ebrazi R. A flexible reformulation of the refueling station location problem. *Transp Sci*. 2013; 47: 617-628.
25. Lin RH, Ye ZZ, Wu BD. A review of hydrogen station location models. *Int J Hydrog Energy*. 2020; 45: 20176-20183.
26. Rezaei M, Alharbi SA, Razmjoo A, Mohamed MA. Accurate location planning for a wind-powered hydrogen refueling station: Fuzzy VIKOR method. *Int J Hydrog Energy*. 2021; 46: 33360-33374.
27. Li Y, Cui F, Li L. An integrated optimization model for the location of hydrogen refueling stations. *Int J Hydrog Energy*. 2018; 43: 19636-19649.
28. Genç MS, Karipoğlu F, Koca K, Azgın ŞT. Suitable site selection for offshore wind farms in Turkey's seas: GIS-MCDM based approach. *Earth Sci Inform*. 2021; 14: 1213-1225.

29. Lin CC, Lin CC. The p-center flow-refueling facility location problem. *Transp Res Part B*. 2018; 118: 124-142.
30. Wang D, Wang Z, Han F, Zhao F, Ji Y. Location optimization of hydrogen refueling stations in hydrogen expressway based on hydrogen supply chain cost. *Front Artif Intell Appl*. 2021; 341: 368-374.
31. Bae S, Lee E, Han J. Multi-period planning of hydrogen supply network for refuelling hydrogen fuel cell vehicles in urban areas. *Sustainability*. 2020; 12: 4114.
32. Kuvvetli Y. Multi-objective and multi-period hydrogen refueling station location problem. *Int J Hydrog Energy*. 2020; 45: 30845-30858.
33. Zhou Y, Qin X, Li C, Zhou J. An intelligent site selection model for hydrogen refueling stations based on fuzzy comprehensive evaluation and artificial neural network-a case study of Shanghai. *Energies*. 2022; 15: 1098.
34. Kim H, Eom M, Kim BI. Development of strategic hydrogen refueling station deployment plan for Korea. *Int J Hydrog Energy*. 2020; 45: 19900-19911.
35. Yang G, Jiang Y. Siting and sizing of the hydrogen refueling stations with on-site water electrolysis hydrogen production based on robust regret. *Int J Energy Res*. 2020; 44: 8340-8361.
36. Hernández B, Alkayas A, Azar E, Mayyas AT. Mathematical model for the placement of hydrogen refueling stations to support future fuel cell trucks. *IEEE Access*. 2021; 9: 148118-148131.
37. Farahani RZ, Asgari N, Heidari N, Hosseini M, Goh M. Covering problems in facility location: A review. *Comput Ind Eng*. 2012; 62: 368-407.
38. Kennedy J, Eberhart R. Particle swarm optimization. *Proceedings of ICNN'95-International Conference on Neural Networks*; 1995 November 27-December 01; Perth, WA, Australia. Piscataway, New Jersey, USA: IEEE.
39. Bruno G, Genovese A, Sgalambro A. An agent-based framework for modeling and solving location problems. *Top*. 2010; 18: 81-96.
40. Melendez M, Milbrandt A. Regional consumer hydrogen demand and optimal hydrogen refueling station siting [Internet]. 2008 [cited date 2023 January 12]. Available from: <http://www.osti.gov/servlets/purl/928253-WOcGno/>.
41. Fúnez Guerra C, García-Ródenas R, Angulo Sánchez-Herrera E, Rayo DV, Clemente-Jul C. Modeling of the behavior of alternative fuel vehicle buyers. A model for the location of alternative refueling stations. *Int J Hydrog Energy*. 2016; 41: 19312-19319.
42. Tostado-Véliz M, Ghadimi AA, Miveh MR, Bayat M, Jurado F. Uncertainty-aware energy management strategies for PV-assisted refuelling stations with onsite hydrogen generation. *J Clean Prod*. 2022; 365: 132869.
43. Berman O, Drezner Z. The p-median problem under uncertainty. *Eur J Oper Res*. 2008; 189: 19-30.
44. Shetab-Boushehri SN, Rajabi P, Mahmoudi R. Modeling location–allocation of emergency medical service stations and ambulance routing problems considering the variability of events and recurrent traffic congestion: A real case study. *Healthcare Anal*. 2022; 2: 100048.
45. Mulvey JM, Beck MP. Solving capacitated clustering problems. *Eur J Oper Res*. 1984; 18: 339-348.
46. Wilensky U. NetLogo [Internet]. 1999. Available from: <http://ccl.northwestern.edu/netlogo/>.
47. Akarsu B, Serdar Genç M. Optimization of electricity and hydrogen production with hybrid renewable energy systems. *Fuel* 2022;324:124465.

48. Genç G, Çelik M, Serdar Genç M. Cost analysis of wind-electrolyzer-fuel cell system for energy demand in Pınarbaşı-Kayseri. *International Journal of Hydrogen Energy* 2012;37:12158-66.
49. Cuevas E, Gálvez J, Avila K, Toski M, Rafe V. A new metaheuristic approach based on agent systems principles. *J Comput Sci.* 2020; 47: 101244.
50. Irawan CA, Imran A, Luis M. Solving the bi-objective capacitated p-median problem with multilevel capacities using compromise programming and VNS. *Int Trans Oper Res.* 2020; 27: 361-380.